

Light dilaton near critical points in top-down holography

Daniel Elander^{1,*}, Antón F. Faedo^{2,3,†}, Maurizio Piai^{4,5,‡}, Ronnie Rodgers^{6,§}, and Javier G. Subils^{7,||}

¹Porto, Portugal

²Departamento de Física, Universidad de Oviedo, c/ Leopoldo Calvo Sotelo 18, ES-33007, Oviedo, Spain

³Instituto Universitario de Ciencias y Tecnologías Espaciales (ICTEA),

Calle de la Independencia 13, ES-33004, Oviedo, Spain

⁴Department of Physics, Faculty of Science and Engineering, Swansea University,

Singleton Park, SA2 8PP, Swansea, Wales, United Kingdom

⁵Centre for Quantum Fields and Gravity, Faculty of Science and Engineering, Swansea University,

Singleton Park, SA2 8PP, Swansea, United Kingdom

⁶Nordita, Stockholm University and KTH Royal Institute of Technology,

Hannes Alfvénsgatan 12, SE-106 91 Stockholm, Sweden

⁷Institute for Theoretical Physics, Utrecht University, 3584 CC Utrecht, The Netherlands



(Received 18 March 2025; accepted 1 December 2025; published 19 December 2025)

We study a class of UV-complete, strongly coupled, confining three-dimensional field theories, that exhibit a novel stabilization mechanism for the mass of the lightest scalar composite state, relying on the existence of a critical point. The theories admit a holographic dual description in terms of regular backgrounds in 11-dimensional supergravity, which retains its rigorous microscopic interpretation in field theory. The phase diagram includes a line of first-order phase transitions ending at the critical point, where the transition becomes of second order. We calculate the mass spectrum of bound states of the field theory, by considering fluctuations around the background solutions, and find that, near the critical point, a hierarchy of scales develops, such that one state becomes parametrically light. We identify this state as the dilaton, the pseudo-Nambu-Goldstone boson associated with the spontaneous breaking of approximate scale invariance, demonstrating the emergence of this composite state in an *ab initio* calculation that has a field theory origin. A stabilization mechanism of this type might be exploited to address hierarchy problems in particle and astroparticle physics.

DOI: 10.1103/1wqc-vk7q

I. INTRODUCTION

One promising approach to the electroweak hierarchy problem of the Standard Model is the idea that the Higgs boson [1,2] might be a composite particle—the dilaton—emerging at low energies, in a new, strongly coupled, confining sector of a more complete theory. In this scenario, the small mass of the Higgs boson, as well as the hierarchy between electroweak and new physics scales, originates from the spontaneous breaking of approximate scale invariance [3]. The striking, experimentally testable implications

of this framework [4] motivate phenomenological and effective field theory studies [5–18]. A stabilization mechanism would ensure that explicit symmetry breaking terms are parametrically small, providing a natural suppression of the dilaton mass, in respect to the strong-coupling scale.

At a microscopic level, the features of such a scenario are less understood [19–22]. Partly, this is due to the challenge of investigating strongly coupled confining physics. A dilaton is expected to appear in the spectrum of bound states if the confining dynamics is influenced by the proximity, in parameter space, to a weak (second-order) phase transition. Yet, a complete, calculable implementation of these ideas is still missing in four-dimensional gauge theories. In this paper, we take a critical step in this direction, by demonstrating these phenomena in a class of confining theories in lower dimensions.

To do so, we rely on gauge-gravity dualities [23–26], which offer an unprecedented opportunity to perform definite computations, linking strongly coupled field theory to weakly coupled gravity in higher dimensions. The physics of confinement in the dual gravity theory is captured by background geometries in which a portion of space shrinks

*Contact author: daniel.elander@gmail.com

†Contact author: anton.faedo@uniovi.es

‡Contact author: m.piai@swansea.ac.uk

§Contact author: ronnie.rodgers@su.se

||Contact author: j.gomezsubils@uu.nl

smoothly [27–33]. The free energy of different field-theory configurations is calculable holographically, providing a means to analyze the phase structure. Similarly, the spectrum of bound states is extracted from the fluctuations of the gravity background, treated with the gauge-invariant formalism developed in Refs. [34–41]. Explorations of possible backgrounds, looking for evidence of a light dilaton, are found in Refs. [42–65].

The relation between the nature of phase transitions and the mass of the lightest state in holography has been studied in models chosen on the basis of simplicity arguments (bottom-up holography) [66,67] as well as consistent truncations of fundamental quantum gravity theories (top down) [68–70]. It has been observed that, in proximity to first-order transitions, the mass of the lightest scalar state in the spectrum is numerically suppressed, although this typically happens in a branch of metastable states. Yet, in the confining bottom-up model of Ref. [71] (Model B), a line of first-order phase transitions terminates at a critical point. In its close proximity, the mass of the lightest scalar particle can be dialed to be parametrically small in stable states of the theory.

Inspired by this result, but within the context of top-down holography, we present the first example of confining field theories in which a light dilaton emerges from the dynamics, in the proximity of a critical point at the end of a line of first-order phase transitions. At variance with the model in Ref. [71], the backgrounds of interest admit a rigorous field-theory dual interpretation, hence filling an important gap in the literature and solving a long-standing problem in field theory. The solutions, constructed within 11-dimensional supergravity, are regular, based on the circle compactification of those reported in Ref. [72], and can be thought of as the double-Wick rotated versions of the solutions constructed in Ref. [73]. We refer to these publications for details and provide only the information necessary to make our presentation self-contained.

II. THE HOLOGRAPHIC MODEL

The truncation detailed in Refs. [62,72,73] consists of six scalars, $\Phi^i = \{\Phi, U, V, a_J, b_J, b_X\}$, coupled to gravity in four dimensions. We further compactify it on a circle, S_ℓ^1 , where ℓ denotes its circumference (for details, see Supplemental Material [74]). The resulting three-dimensional, classical theory consists of gravity coupled to a sigma model with seven scalars, $\Phi^a = \{\Phi^i, \chi\}$, and a $U(1)$ gauge field, A_M . The action is

$$\mathcal{S}_3 = \frac{2}{\kappa_3^2} \int d^3x \sqrt{|g|} \left[\frac{R}{4} - \frac{1}{2} G_{ab}(\Phi^c) \partial^M \Phi^a \partial_M \Phi^b - \frac{e^{-4\chi}}{16} F_{MN} F^{MN} - \mathcal{V}(\Phi^a) \right]. \quad (1)$$

The metric, g_{MN} , with spacetime indices $M = 0, 1, 2$, has signature mostly “+,” determinant g , and Ricci scalar R .

The field-strength tensor is $F_{MN} \equiv \partial_M A_N - \partial_N A_M$, and scalar field indices are lowered with the sigma-model metric, G_{ab} , defined as

$$\begin{aligned} G_{ab} d\Phi^a d\Phi^b = & \frac{1}{4} d\Phi^2 + 2dU^2 + 6dV^2 + 4dUdV + d\chi^2 \\ & + 2e^{-4V-\Phi} db_J^2 + 4e^{-4U-\Phi} db_X^2 \\ & + 16e^{-2U-4V+\frac{\Phi}{2}} da_J^2. \end{aligned} \quad (2)$$

Finally, the potential is $\mathcal{V} = e^{2\chi} \mathcal{V}_4(\Phi^i)$ with¹

$$\begin{aligned} \mathcal{V}_4 = & 8(b_J + b_X)^2 e^{-4U-8V-\Phi} - 6e^{-2U-6V} - 2e^{-4U-4V} \\ & + \frac{1}{2} e^{-8V} + 16[2a_J + Q_k(b_J - b_X) - q_c]^2 e^{-6U-8V+\frac{\Phi}{2}} \\ & + 8(2a_J - Q_k b_J + q_c)^2 e^{-2U-12V+\frac{\Phi}{2}} + Q_k^2 e^{-2U-8V+\frac{3\Phi}{2}} \\ & + 2Q_k^2 e^{-6U-4V+\frac{3\Phi}{2}} + 32e^{-6U-12V-\frac{\Phi}{2}} [4a_J(b_J + b_X) \\ & + Q_k b_J(b_J - 2b_X) + 2q_c(b_X - b_J)]^2. \end{aligned} \quad (3)$$

The parameters Q_k and q_c appear in the fluxes of the uplifted solutions, which are dual to three-dimensional $U(N)_k \times U(N+M)_{-k}$ quiver gauge theories with Chern-Simons interactions at level k . With the shorthand notation $\bar{M} \equiv M - k/2$, we have (see Ref. [72])

$$q_c = \frac{3\pi\ell_s^3 g_s}{4} \bar{M}, \quad Q_k = \frac{\ell_s g_s}{2} k, \quad (4)$$

with ℓ_s and g_s the string length and coupling, respectively. Combining these expressions with the 't Hooft coupling of the microscopic theory, $\lambda = \ell_s^{-1} g_s N$, the gauge theory depends on a scale, Λ , which we use to set the scale of dimensionful quantities, and a parameter, α ,

$$\Lambda = \frac{k^2 \lambda}{6\pi N \bar{M}}, \quad \alpha = \frac{9\bar{M}^3}{256|k|\pi}. \quad (5)$$

The system of nonlinear equations derived from this action admit a rich space of (nonsupersymmetric) background solutions lifting to regular geometries in 11 dimensions—see Refs. [72,73]. These solutions encapsulate the renormalization group flow of a family of dual field theories. The action and space of solutions are rigidly determined, both by the string theory construction and by the properties of the dual field theories. The solutions can be labeled by two additional parameters: the circumference, ℓ , of the circle, S_ℓ^1 , and $b_0 \in (0, 1)$, which is related to the asymptotic value of the scalar b_J —see Eq. (12) in Supplemental Material [74]—and encodes the relative difference in the (inverse squared) gauge coupling of the two groups in the quiver. In the following, we describe the different phases in the space of these two parameters and

¹Compared to Refs. [62,72,73], we set $Q_c = 0$, following Ref. [75].

highlight the key features of the phase transitions that separate them.

III. PHASE DIAGRAM AND PHASE TRANSITIONS

Each choice of the dimensionless pair $(\ell\Lambda, b_0)$ identifies a solution that is regular when uplifted to 11-dimensional supergravity and in which the size of the circle S_ℓ^1 is nonzero everywhere. The dual is a three-dimensional *nonconfining* state of the field theory, as the quark-antiquark potential is screened [72]. In a region of $(\ell\Lambda, b_0)$ space there are also alternative solutions for which S_ℓ^1 shrinks smoothly to zero size, providing the dual to a *confining* state. With choices of $(\ell\Lambda, b_0)$ for which both solutions exist, the one with the lowest free energy is preferred.

The calculation of the free energy, via holographic renormalization [76–78] (see Supplemental Material [74] for the relevant formulas), leads to the identification of three types of phase transitions. In the range $b_0 \in (b_0^{\text{CP}}, b_0^{\text{triple}}) \simeq (0.6815, 0.6847)$, the free energy is a multivalued function of $\ell\Lambda$ —see Fig. 1 (left). A first-order phase transition connects different confining solutions. A discontinuity appears in the response function, $\langle T_{22} \rangle$, the expectation value of the component of the energy-momentum tensor along S_ℓ^1 —see the right panel of Fig. 1. A line of such first-order transitions exists, represented by the dashed black line in Fig. 2. As b_0 approaches b_0^{CP} , the transition weakens and eventually disappears into a smooth crossover—see Fig. 3 (left).

Phase transitions between confining and nonconfining states (with zero free energy) also exist, for all values of $b_0 \in (0, 1)$ —see Figs. 4 and 5. If $b_0 < b_0^{\text{triple}}$, the phase transition is such that the free energy of the confining phase touches tangent to the horizontal axes (represented by the hollow orange disk in the top panel of Fig. 1), as in second order phase transitions. However, its true nature is difficult to determine, since close to this particular line, the

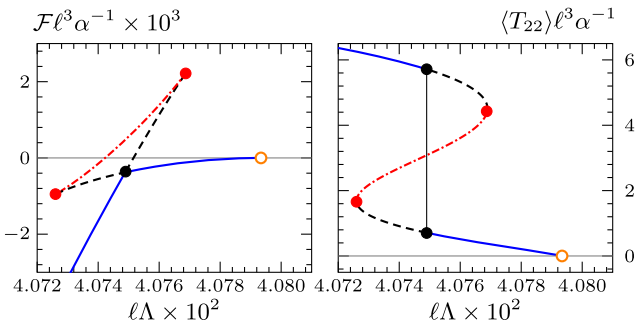


FIG. 1. Free energy density, $\mathcal{F}\ell^3$ (left panel), and response function, $\langle T_{22} \rangle\ell^3$ (right panel), as functions of the circumference, $\ell\Lambda$, of the compact dimension for confining solutions with the representative choice $b_0 = 0.6836$. The solid black disks indicate the location of a first-order phase transition between two different confining solutions. Beyond the hollow orange disk nonconfining solutions are energetically favored.

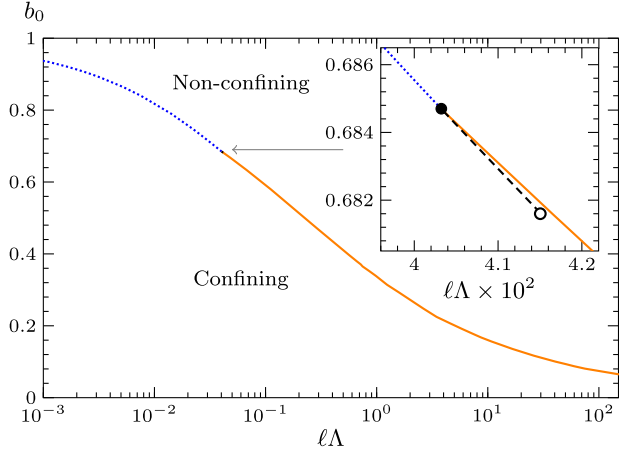


FIG. 2. Phase diagram of the system. Dotted blue and solid orange curves separate confined and nonconfined phases, the former identifying first-order phase transitions. Details of the region near the triple point, $b_0^{\text{triple}} \simeq 0.6847$ (black disk), are shown in the inset panel. A line of first-order phase transitions (dashed black) between different confined states joins b_0^{triple} to the critical point at $b_0^{\text{CP}} \simeq 0.6815$ (white disk).

geometries become increasingly curved. In contrast, for $b_0 > b_0^{\text{triple}}$ the curve crosses the axes and the phase transition is of first order. All these cases are summarized in the phase diagram in Fig. 2.

The region of parameter space in proximity to the orange line in Fig. 2 is the only one in which the classical supergravity approximation breaks down. In the rest of the parameter space, quantum gravity and stringy corrections can be safely neglected, as all curvature invariant are finite, and suppressed in the appropriate large- N limit (see Ref. [73] for details).

IV. MASS SPECTRA OF FLUCTUATIONS

The left panels of Fig. 3 show that the confining solutions are uniquely labeled by the pair $(b_0, \langle T_{22} \rangle\ell^3\alpha^{-1})$. We compute the spectrum of small fluctuations of the sigma model coupled to gravity around the confining solutions, by exploiting the gauge-invariant approach of Refs. [34–41]. The linearized fluctuation equations for the metric, scalar, and vector fields reduce to coupled equations for seven gauge-invariant scalar fluctuations, α^a , and one vector fluctuation, \mathbf{v} .

The spectrum of (squared) masses for the fluctuations is obtained by solving the linearized equations, subject to the requirement that their leading-order modes vanish, both asymptotically, in the ultraviolet (UV) regime of the field theory, and at the end of space, corresponding to the infrared (IR).

We numerically determine these masses, m^2 , using a pseudospectral method [79]. We approximate the solutions as a series of the first K Chebyshev polynomials of the first kind, and evaluate the equations and boundary

conditions on the Gauss-Lobatto grid. This approximates the differential equation as a matrix eigenvalue problem. The eigenvalues, m^2 , are extracted using *Mathematica*'s eigenvalue solver. To check convergence of the numerics, we compute the eigenvalues for different values of K , keeping only those that agree between the computations. More details on our numerical procedure are given in Supplemental Material [74].

V. RESULTS

Our main result is the appearance of a parametrically light scalar, which we identify as a dilaton, in the region of

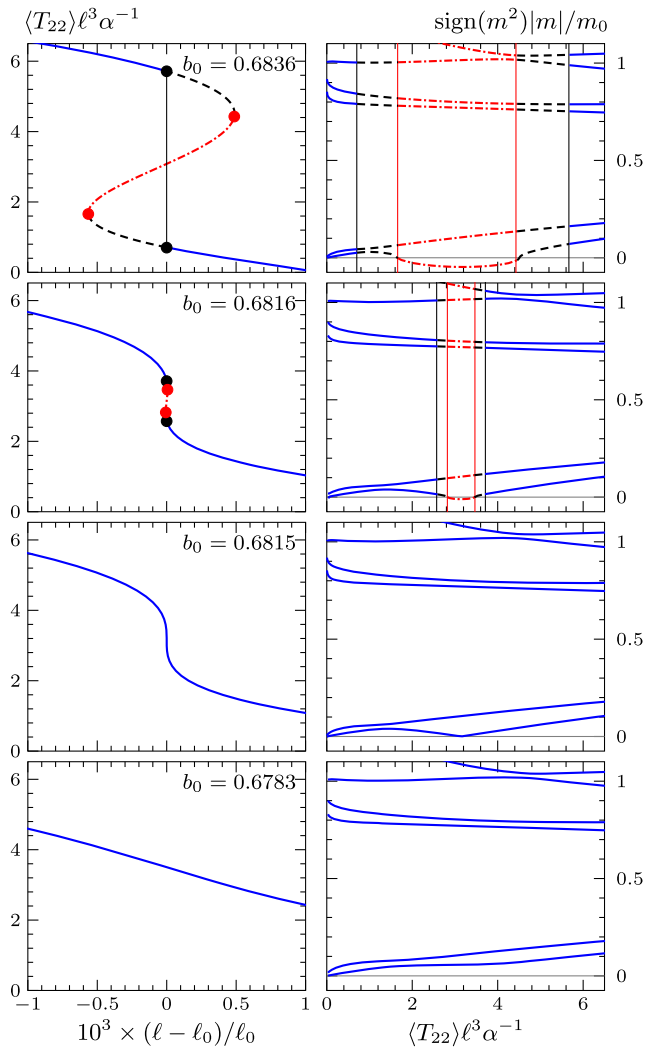


FIG. 3. Left panels: component of the stress tensor in the compact direction, $\langle T_{22} \rangle \ell^3 \alpha^{-1}$, as a function of its size, ℓ , for representative values of b_0 . For values of b_0 such that there is a first-order phase transition we define ℓ_0 as the value of ℓ at the phase transition. When there is no transition, we instead define ℓ_0 as the value of ℓ for which $\langle T_{22} \rangle \ell^3 \alpha^{-1}$ is the steepest. The range of parameters plotted is chosen to cluster around the line of first-order phase transitions denoted by black dashed lines in Fig. 1. Right column: mass spectrum of scalar fluctuations, m , in units of the lightest vector mass, m_0 , in the backgrounds of the left panels.

parameter space close to the critical point at the end of a line of first-order phase transitions. This can be seen in Fig. 3, in which we show the spectrum obtained for four different values of $b_0 \sim b_0^{\text{CP}}$. When a first-order phase transition is present, the spectrum contains a tachyon along the (locally) unstable branch, as seen in the first and second rows of panels. In contrast, when the critical point is reached (third row), the tachyon disappears, and an exactly massless state is realized. The mass of this state becomes positive and rises as b_0 decreases below b_0^{CP} , when the transition becomes a smooth crossover, as in the last row. Our results thus confirm the statement made in Ref. [71] that a light dilaton is expected near a second-order phase transition, and we explicitly find it in a top-down holographic setup with regular geometry.

Having demonstrated that the presence of a critical point suppresses the mass of the lightest scalar state, compared to the other scales and masses, we turn attention to its nature. To this purpose, we repeat the calculation of the spectrum of fluctuations of the confining backgrounds, by introducing a drastic approximation: we ignore the mixing of fluctuations of the sigma-model fields with the trace of the metric, adopting the probe approximation as defined in Ref. [41]. As the trace of the metric couples to the trace of the stress-energy tensor of the dual field theory (the dilatation operator), when the probe approximation fails to capture the lightest scalar state, this signals its (approximate) dilaton nature. We report the results in Fig. 6, for $b_0 = b_0^{\text{CP}}$, as a function of $\langle T_{22} \rangle \ell^3 \alpha^{-1}$.

The probe approximation works well overall, but fails qualitatively in two important respects. First, it misses one tower of bound states, replacing it by a continuum, which we removed from the numerical results with appropriate choices of boundary conditions. Second, it fails to capture the lightest scalar state, in the region of $(b_0, \langle T_{22} \rangle \ell^3 \alpha^{-1})$ close to criticality, thus demonstrating that this state is an approximate dilaton.

The richness provided by the top-down holographic framework adds additional structure to the spectrum of the theory, compared to the bottom-up model from

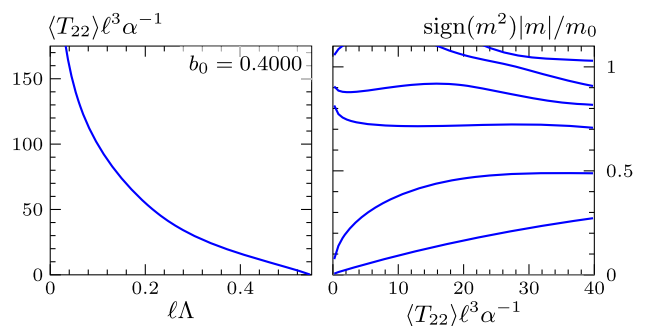


FIG. 4. Response function, $\langle T_{22} \rangle \ell^3 \alpha^{-1}$ (left), and scalar spectrum (right) for a value of $b_0 < b_0^{\text{CP}}$ chosen well below the critical point. Large values of $\ell \Lambda$ approach the boundary between confining and nonconfining configurations.

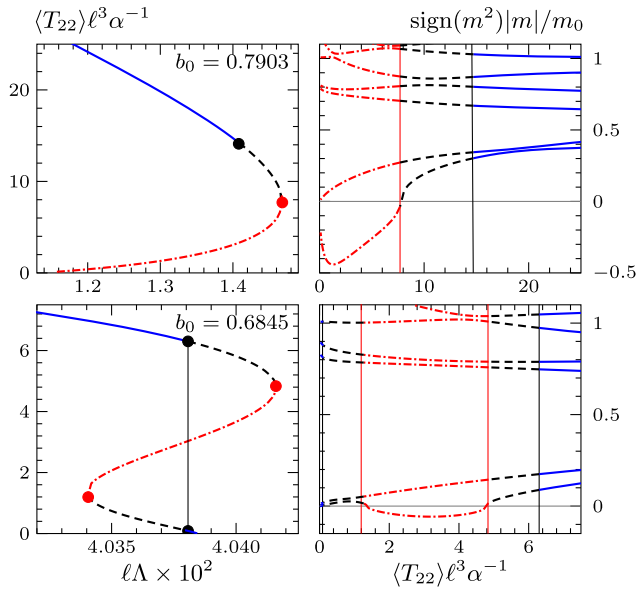


FIG. 5. Response functions, $\langle T_{22} \rangle \ell^3 \alpha^{-1}$ (left), and scalar spectrum (right) for values of $b_0 > b_0^{\text{CP}}$, so that a first-order phase transition appears. The top row shows a representative case well above the critical point, where the first-order phase transition is between confining and nonconfining solutions. In the bottom row $b_0 \simeq b_0^{\text{triple}}$, slightly below the triple point.

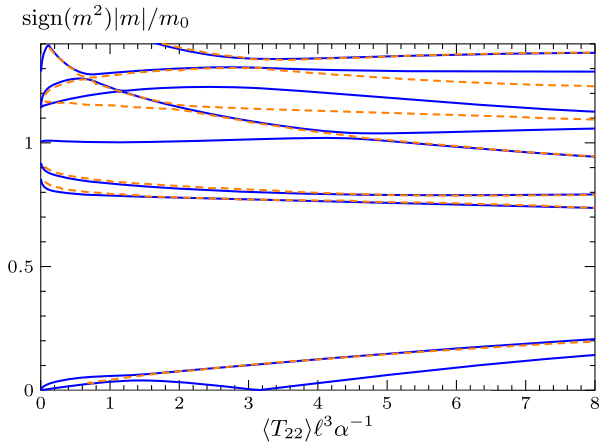


FIG. 6. Mass spectrum of scalar fluctuations computed for $b_0 = 0.6815$, as in the third row of Fig. 3 (solid blue), and in the probe approximation (dashed orange), which neglects the effect of the trace of the three-dimensional metric. The probe approximation fails to capture the light mode that appears close to criticality, the dilaton.

Ref. [71]. Besides the appearance of a light dilaton near the critical point, the most striking feature is the appearance of a second, additional light state, for $b_0 \in (0, b_0^{\text{triple}})$, when the order parameter, $\langle T_{22} \rangle$, is small—see Figs. 3 and 4. As is apparent from Fig. 6, the probe approximation describes well one of these light states, which is hence not related to the dilaton. This region of parameter space corresponds to

approaching the solid orange line separating confining and nonconfining backgrounds in Fig. 2. Unfortunately, when $\langle T_{22} \rangle \rightarrow 0$, the geometry becomes strongly curved, and eventually singular, preventing us from drawing firm conclusions about this separated, interesting region.

In contrast, for $b_0 > b_0^{\text{triple}}$, the masses of the states are never suppressed along the stable branch—see Fig. 5 (top). For completeness, we show in Fig. 5 (bottom) the spectrum near the special case of the triple point, $b_0 \simeq b_0^{\text{triple}}$, at which the end of the metastable branch touches the first-order phase transition corresponding to the dashed, black line in Fig. 2.

VI. OUTLOOK

We exhibited a top-down holographic description of three-dimensional strongly coupled theories in which the mass of a light dilaton state is naturally suppressed by the existence of a nearby critical point in parameter space, putting the results of Ref. [71] on firm field-theory footing (see also the recent Ref. [80], and the lattice study in Ref. [81]). The emergence of a parametrically light dilaton in a confining theory, accompanied by a hierarchy of dynamically generated scales, has been advocated as a way to address hierarchy problems, in the electroweak theory as well as in extensions of the standard model, hence our results have a range of potential applications.

It would be interesting to implement this mechanism in four or higher number of dimensions. If examples exist with the additional feature that other approximate symmetries are also spontaneously broken, one could further link our findings with dilaton effective field theory (dEFT), in which the dilaton couples to light composite pseudo-Nambu-Goldstone bosons (PNGBs) [82–95]. It would also be interesting to investigate possible applications in lower-dimensional field theory, as suggested in Ref. [80], particularly in the context of conformal perturbation theory—see, e.g., Refs. [96–99]. Applications of dEFT range from the analysis of special lattice theories [100], to new dark matter proposals [101] to composite Higgs models in which also the Higgs boson is a PNGB [102–104], as suggested in Refs. [105,106], by elaborating on Refs. [107–109]—see the reviews [110–114] and the tables in Refs. [115–117].

The essential finding of the paper is related to the existence of lines of first-order transitions, with end points, and hence a possible strategy for this search would involve applying existing solution-generating techniques, as those discussed in Ref. [118], to produce new families of supergravity solutions labeled by more than one parameter.

ACKNOWLEDGMENTS

We thank Carlos Hoyos for discussions and collaboration in early stages of this project. We thank David Mateos for discussions. A. F. is partially supported by the AEI and the MCIU through the Spanish Grant No. PID2021-123021NB-I00. The work of M. P. has

been supported by the STFC Consolidated Grants No. ST/T000813/1 and No. ST/X000648/1. M. P. received funding from the European Research Council (ERC) under the European Union's Horizon 2020 research and innovation program under Grant Agreement No. 813942. The work of R. R. was supported by the European Union's Horizon Europe research and innovation program under Marie Skłodowska-Curie Grant Agreement No. 101104286. Nordita is supported

in part by Nordforsk. J. S. thanks Nordita and Lärkstadens Studiecentrum for their hospitality during his stay in Stockholm from October 9 to 16, 2024, when the main part of this project was undertaken.

DATA AVAILABILITY

The data that support the findings of this article are openly available [119].

[1] G. Aad *et al.* (ATLAS Collaboration), *Phys. Lett. B* **716**, 1 (2012).

[2] S. Chatrchyan *et al.* (CMS Collaboration), *Phys. Lett. B* **716**, 30 (2012).

[3] S. Coleman, *Aspects of Symmetry: Selected Erice Lectures* (Cambridge University Press, Cambridge, England, 1985).

[4] W. D. Goldberger, B. Grinstein, and W. Skiba, *Phys. Rev. Lett.* **100**, 111802 (2008).

[5] D. K. Hong, S. D. H. Hsu, and F. Sannino, *Phys. Lett. B* **597**, 89 (2004).

[6] D. D. Dietrich, F. Sannino, and K. Tuominen, *Phys. Rev. D* **72**, 055001 (2005).

[7] L. Vecchi, *Phys. Rev. D* **82**, 076009 (2010).

[8] M. Hashimoto and K. Yamawaki, *Phys. Rev. D* **83**, 015008 (2011).

[9] L. Del Debbio and R. Zwicky, *J. High Energy Phys.* **08** (2022) 007.

[10] R. Zwicky, [arXiv:2306.12914](https://arxiv.org/abs/2306.12914).

[11] R. Zwicky, *Phys. Rev. D* **110**, 014048 (2024).

[12] E. Eichten, K. Lane, and A. Martin, [arXiv:1210.5462](https://arxiv.org/abs/1210.5462).

[13] D. Elander and M. Piai, *Nucl. Phys.* **B867**, 779 (2013).

[14] Z. Chacko and R. K. Mishra, *Phys. Rev. D* **87**, 115006 (2013).

[15] B. Bellazzini, C. Csaki, J. Hubisz, J. Serra, and J. Terning, *Eur. Phys. J. C* **73**, 2333 (2013).

[16] T. Abe, R. Kitano, Y. Konishi, K.-y. Oda, J. Sato, and S. Sugiyama, *Phys. Rev. D* **86**, 115016 (2012).

[17] B. Bellazzini, C. Csaki, J. Hubisz, J. Serra, and J. Terning, *Eur. Phys. J. C* **74**, 2790 (2014).

[18] P. Hernandez-Leon and L. Merlo, *Phys. Rev. D* **96**, 075008 (2017).

[19] B. Holdom and J. Terning, *Phys. Lett. B* **187**, 357 (1987).

[20] B. Holdom and J. Terning, *Phys. Lett. B* **200**, 338 (1988).

[21] T. Appelquist and Y. Bai, *Phys. Rev. D* **82**, 071701 (2010).

[22] B. Grinstein and P. Uttayarat, *J. High Energy Phys.* **07** (2011) 038.

[23] J. M. Maldacena, *Adv. Theor. Math. Phys.* **2**, 231 (1998).

[24] S. S. Gubser, I. R. Klebanov, and A. M. Polyakov, *Phys. Lett. B* **428**, 105 (1998).

[25] E. Witten, *Adv. Theor. Math. Phys.* **2**, 253 (1998).

[26] O. Aharony, S. S. Gubser, J. M. Maldacena, H. Ooguri, and Y. Oz, *Phys. Rep.* **323**, 183 (2000).

[27] E. Witten, *Adv. Theor. Math. Phys.* **2**, 505 (1998).

[28] I. R. Klebanov and M. J. Strassler, *J. High Energy Phys.* **08** (2000) 052.

[29] J. M. Maldacena and C. Nunez, *Phys. Rev. Lett.* **86**, 588 (2001).

[30] A. Butti, M. Graña, R. Minasian, M. Petrini, and A. Zaffaroni, *J. High Energy Phys.* **03** (2005) 069.

[31] C. Nunez, M. Oyarzo, and R. Stuardo, *J. High Energy Phys.* **03** (2024) 080.

[32] D. Chatzis, A. Fatemiabhari, C. Nunez, and P. Weck, *Nucl. Phys.* **B1006**, 116659 (2024).

[33] D. Chatzis, A. Fatemiabhari, C. Nunez, and P. Weck, *J. High Energy Phys.* **08** (2024) 041.

[34] M. Bianchi, M. Prisco, and W. Mueck, *J. High Energy Phys.* **11** (2003) 052.

[35] M. Berg, M. Haack, and W. Mueck, *Nucl. Phys. B* **736**, 82 (2006).

[36] M. Berg, M. Haack, and W. Mueck, *Nucl. Phys. B* **789**, 1 (2008).

[37] D. Elander, *J. High Energy Phys.* **03** (2010) 114.

[38] D. Elander and M. Piai, *J. High Energy Phys.* **01** (2011) 026.

[39] D. Elander, *Phys. Rev. D* **91**, 126012 (2015).

[40] D. Elander, M. Piai, and J. Roughley, *J. High Energy Phys.* **02** (2019) 101.

[41] D. Elander, M. Piai, and J. Roughley, *J. High Energy Phys.* **06** (2020) 177; **12** (2020) 109(E).

[42] W. D. Goldberger and M. B. Wise, *Phys. Rev. Lett.* **83**, 4922 (1999).

[43] O. DeWolfe, D. Z. Freedman, S. S. Gubser, and A. Karch, *Phys. Rev. D* **62**, 046008 (2000).

[44] W. D. Goldberger and M. B. Wise, *Phys. Lett. B* **475**, 275 (2000).

[45] C. Csaki, M. L. Graesser, and G. D. Kribs, *Phys. Rev. D* **63**, 065002 (2001).

[46] N. Arkani-Hamed, M. Porrati, and L. Randall, *J. High Energy Phys.* **08** (2001) 017.

[47] R. Rattazzi and A. Zaffaroni, *J. High Energy Phys.* **04** (2001) 021.

[48] L. Kofman, J. Martin, and M. Peloso, *Phys. Rev. D* **70**, 085015 (2004).

[49] D. Elander, C. Nunez, and M. Piai, *Phys. Lett. B* **686**, 64 (2010).

[50] D. Elander and M. Piai, *Nucl. Phys.* **B864**, 241 (2012).

[51] D. Elander and M. Piai, *Nucl. Phys.* **B871**, 164 (2013).

[52] D. Kutasov, J. Lin, and A. Parnachev, *Nucl. Phys. B* **863**, 361 (2012).

[53] N. Evans and K. Tuominen, *Phys. Rev. D* **87**, 086003 (2013).

[54] D. Elander, A. F. Faedo, C. Hoyos, D. Mateos, and M. Piai, *J. High Energy Phys.* **05** (2014) 003.

[55] C. Hoyos, U. Kol, J. Sonnenschein, and S. Yankielowicz, *J. High Energy Phys.* **10** (2013) 181.

[56] E. Megias and O. Pujolas, *J. High Energy Phys.* **08** (2014) 081.

[57] D. Elander, R. Lawrence, and M. Piai, *Nucl. Phys. B* **897**, 583 (2015).

[58] E. Megias, O. Pujolas, and M. Quiros, *EPJ Web Conf.* **126**, 05010 (2016).

[59] A. Athenodorou, E. Bennett, G. Bergner, D. Elander, C. J. D. Lin, B. Lucini, and M. Piai, *J. High Energy Phys.* **06** (2016) 114.

[60] D. Elander and M. Piai, *Phys. Lett. B* **772**, 110 (2017).

[61] D. Elander and M. Piai, *J. High Energy Phys.* **06** (2017) 003.

[62] D. Elander, A. F. Faedo, D. Mateos, D. Pravos, and J. G. Subils, *J. High Energy Phys.* **05** (2019) 175.

[63] A. Pomarol, O. Pujolas, and L. Salas, *J. High Energy Phys.* **10** (2019) 202.

[64] J. Cruz Rojas, D. K. Hong, S. H. Im, and M. Järvinen, *J. High Energy Phys.* **05** (2023) 204.

[65] A. Pomarol and L. Salas, *J. High Energy Phys.* **08** (2024) 149.

[66] D. Elander, A. Fatemiabhari, and M. Piai, *Phys. Rev. D* **108**, 015021 (2023).

[67] A. Fatemiabhari, C. Nunez, M. Piai, and J. Rucinski, *Phys. Rev. D* **111**, 066009 (2025).

[68] D. Elander, M. Piai, and J. Roughley, *Phys. Rev. D* **103**, 106018 (2021).

[69] D. Elander, M. Piai, and J. Roughley, *Phys. Rev. D* **103**, 046009 (2021).

[70] D. Elander, M. Piai, and J. Roughley, *Phys. Rev. D* **104**, 046003 (2021).

[71] A. F. Faedo, C. Hoyos, M. Piai, R. Rodgers, and J. G. Subils, *Phys. Rev. D* **110**, 126017 (2024).

[72] A. F. Faedo, D. Mateos, D. Pravos, and J. G. Subils, *J. High Energy Phys.* **06** (2017) 153.

[73] D. Elander, A. F. Faedo, D. Mateos, and J. G. Subils, *J. High Energy Phys.* **06** (2020) 131.

[74] See Supplemental Material at <http://link.aps.org/supplemental/10.1103/1wqc-vk7q> for details of the holographic model, including equations of motion and boundary conditions for fluctuations, and details of our numerical procedure.

[75] A. F. Faedo, C. Hoyos, and J. G. Subils, *J. High Energy Phys.* **03** (2023) 218.

[76] M. Bianchi, D. Z. Freedman, and K. Skenderis, *Nucl. Phys.* **B631**, 159 (2002).

[77] K. Skenderis, *Classical Quantum Gravity* **19**, 5849 (2002).

[78] I. Papadimitriou and K. Skenderis, *IRMA Lect. Math. Theor. Phys.* **8**, 73 (2005).

[79] J. P. Boyd, *Chebyshev and Fourier Spectral Methods* (Springer, Berlin, Heidelberg, 1989).

[80] C. Cresswell-Hogg, D. F. Litim, and R. Zwicky, [arXiv:2502.00107](https://arxiv.org/abs/2502.00107).

[81] B. Lucini, A. Patella, A. Rago, and E. Rinaldi, *J. High Energy Phys.* **11** (2013) 106.

[82] S. Matsuzaki and K. Yamawaki, *Phys. Rev. Lett.* **113**, 082002 (2014).

[83] M. Golterman and Y. Shamir, *Phys. Rev. D* **94**, 054502 (2016).

[84] A. Kasai, K.-i. Okumura, and H. Suzuki, [arXiv:1609.02264](https://arxiv.org/abs/1609.02264).

[85] M. Hansen, K. Langæble, and F. Sannino, *Phys. Rev. D* **95**, 036005 (2017).

[86] M. Golterman and Y. Shamir, *Phys. Rev. D* **95**, 016003 (2017).

[87] T. Appelquist, J. Ingoldby, and M. Piai, *J. High Energy Phys.* **07** (2017) 035.

[88] T. Appelquist, J. Ingoldby, and M. Piai, *J. High Energy Phys.* **03** (2018) 039.

[89] O. Catà, R. J. Crewther, and L. C. Tunstall, *Phys. Rev. D* **100**, 095007 (2019).

[90] M. Golterman and Y. Shamir, *Phys. Rev. D* **98**, 056025 (2018).

[91] O. Catà and C. Müller, *Nucl. Phys.* **B952**, 114938 (2020).

[92] T. Appelquist, J. Ingoldby, and M. Piai, *Phys. Rev. D* **101**, 075025 (2020).

[93] M. Golterman, E. T. Neil, and Y. Shamir, *Phys. Rev. D* **102**, 034515 (2020).

[94] M. Golterman and Y. Shamir, *Phys. Rev. D* **102**, 114507 (2020).

[95] T. Appelquist, J. Ingoldby, and M. Piai, *Universe* **9**, 10 (2023).

[96] G. K. Karananas and M. Shaposhnikov, *Phys. Rev. D* **97**, 045009 (2018).

[97] G. Cuomo, L. Rastelli, and A. Sharon, *J. High Energy Phys.* **12** (2024) 144.

[98] M. R. Gaberdiel, A. Konechny, and C. Schmidt-Colinet, *J. Phys. A* **42**, 105402 (2009).

[99] Z. Komargodski and D. Simmons-Duffin, *J. Phys. A* **50**, 154001 (2017).

[100] T. Appelquist *et al.* (LSD Collaboration), *Phys. Rev. D* **108**, L091505 (2023).

[101] T. Appelquist, J. Ingoldby, and M. Piai, *Phys. Rev. D* **110**, 035013 (2024).

[102] D. B. Kaplan and H. Georgi, *Phys. Lett.* **136B**, 183 (1984).

[103] H. Georgi and D. B. Kaplan, *Phys. Lett.* **145B**, 216 (1984).

[104] M. J. Dugan, H. Georgi, and D. B. Kaplan, *Nucl. Phys.* **B254**, 299 (1985).

[105] T. Appelquist, J. Ingoldby, and M. Piai, *Phys. Rev. Lett.* **126**, 191804 (2021).

[106] T. Appelquist, J. Ingoldby, and M. Piai, *Nucl. Phys.* **B983**, 115930 (2022).

[107] L. Vecchi, *J. High Energy Phys.* **02** (2017) 094.

[108] T. Ma and G. Cacciapaglia, *J. High Energy Phys.* **03** (2016) 211.

[109] D. Buarque Franzosi, G. Cacciapaglia, and A. Deandrea, *Eur. Phys. J. C* **80**, 28 (2020).

[110] R. Contino, in *Physics of the Large and the Small* (World Scientific, Singapore, 2011), pp. 235–306.

[111] G. Panico and A. Wulzer, *Lect. Notes Phys.* **913**, 1 (2016).

[112] O. Witzel, *Proc. Sci. LATTICE2018* (2019) 006 [[arXiv:1901.08216](https://arxiv.org/abs/1901.08216)].

- [113] G. Cacciapaglia, C. Pica, and F. Sannino, *Phys. Rep.* **877**, 1 (2020).
- [114] E. Bennett, J. Holligan, D. K. Hong, H. Hsiao, J.-W. Lee, C. J. D. Lin, B. Lucini, M. Mesiti, M. Piai, and D. Vadacchino, *Universe* **9**, 236 (2023).
- [115] G. Ferretti and D. Karateev, *J. High Energy Phys.* 03 (2014) 077.
- [116] G. Ferretti, *J. High Energy Phys.* 06 (2016) 107.
- [117] G. Cacciapaglia, G. Ferretti, T. Flacke, and H. Serôdio, *Front. Phys.* **7**, 22 (2019).
- [118] A. Anabalón and S. F. Ross, *J. High Energy Phys.* 07 (2021) 015.
- [119] D. Elander, A. Faedo, M. Piai, R. Rodgers, and J. Subils, Light dilaton near critical points in top-down holography —data release (2025), [10.5281/zenodo.15004579](https://doi.org/10.5281/zenodo.15004579).